Hindawi Publishing Corporation
Mathematical Problems in Engineering
Volume 2015, Article ID 387368, 8 pages
http://dx.doi.org/10.1155/2015/387368

Research Article

Semianalytical Solution of the Nonlinear Dual-Porosity Flow Model with the Quadratic Pressure Gradient Term

Jiang-Tao Li,[1,2] Ren-Shi Nie,[1] Yong-Lu Jia,[1] and Dan-Ling Wang[1]

[1]*State Key Laboratory of Oil & Gas Reservoir Geology and Exploitation, Southwest Petroleum University, Chengdu 610500, China*
[2]*Petrochina Qinghai Oilfield Company, Dunhuang 736200, China*

Correspondence should be addressed to Ren-Shi Nie; nierenshi2000@126.com

Received 1 August 2014; Accepted 15 January 2015

Academic Editor: Chia-Cheng Tsai

The nonlinear dual-porosity flow model, specifically considering the quadratic pressure gradient term, wellbore storage coefficient, well skin factor, and interporosity flow of matrix to natural fractures, was established for well production in a naturally fractured formation and then solved using a semianalytical method, including Laplace transform and a transformation of the pressure function. Analytical solution of the model in Laplace space was converted to numerical solution in real space using Stehfest numerical inversion. Nonlinear flow process for well production in a naturally fractured formation with different external boundaries was simulated and analyzed using standard pressure curves. Influence of the quadratic pressure gradient coefficient on pressure curves was studied qualitatively and quantitatively in conditions of a group of fixed model parameters. The research results show that the semianalytical modelling method is applicable in simulating the nonlinear dual-porosity flow behavior.

1. Introduction

The fluid flow in porous media was proved to be of nonlinearity [1–3]. The nonlinear flow models with the quadratic pressure gradient term for well production in underground formations were especially investigated in the past. Early in 1989, a steady-state and semisteady-state flow model with the quadratic pressure gradient term was presented [4]. In 1991, a transient flow model with the quadratic gradient term was established and solved [5]. In 1993, the pressure distribution of a radial flow model with the quadratic gradient term was studied and plotted [6, 7]. In 1994, a nonlinear flow model for a dual-porosity formation was established [8, 9]. In 1996, the analytic solution to the nonlinear diffusion equation with the quadratic pressure gradient by considering a constant compressibility of fluid was derived [10]. In 1998, the solutions between linear and nonlinear models were compared [11] and a special nonlinear model for variable-rate well-tests was especially researched [12]. In 2004, the exact solution of a flow model with the quadratic gradient term by considering wellbore storage effect was deduced [13]. In 2005, a fractal model with the quadratic gradient term was presented [14]. In 2008, a class of nonlinear type equations for porous flow was especially proved to be of existence using mathematical theory [2]. In 2009, the nonlinear equation of pressure diffusion was solved using a Hopf-Cole transformation [15]. In 2010, a spherical flow model for a partial perforation well in a formation with a larger thickness was established [16]. In 2013, the effects of the quadratic gradient term on the pressure curves and pressure derivative curves were analyzed qualitatively and quantitatively for homogenous and multiple-zone composite reservoirs [17–19]. Despite copious literatures on the nonlinear flow subject with the quadratic pressure gradient term, most of them were focused on the single porosity medium and only two papers [8, 9] studied the dual-porosity media; however the nonlinear dual-porosity flow model of Bai suffered some limitations in face of the real world: (1) well skin and wellbore storage effects that actually exist in every real well were not considered in his model; (2) a standard set of log-log type curves for nonlinear flow process analysis was not developed; (3) quantitative difference between nonlinear and linear models was not compared. Therefore, the main task of this paper is to address the three issues and clearly show the readers the nonlinear dual-porosity flow behavior in a different way.

2. Physical Model

Physical model assumptions are as follows.

(1) For a single well production at constant rate in an underground dual-porosity formation saturated by a single-phase liquid (oil or water), the external boundary of formation may be infinite or closed or constant pressure.

(2) Underground dual-porosity formation is constructed by natural fracture system and matrix system. It is supposed that fracture permeability is far larger than matrix permeability, so the flow pathway directly connected with wellbore is considered as fracture system.

(3) Slightly compressible rock and liquid with a constant compressibility are considered.

(4) The porous flow is isothermal and conforms to Darcy's law and the gravity and capillary forces are ignored for the flow, and the effect of pressure on fluid viscosity is also ignored for the flow.

(5) Skin effect is considered (near the wellbore where the formation could be damaged by drilling and completion operations there would be an additional pressure drop during production, with the "skin" being a reflection of additional pressure drop).

(6) Wellbore storage effect is considered (in the beginning of opening well, the fluid stored in wellbore starts to flow, and the fluid in the formation does not flow).

(7) At time $t = 0$, pressure is uniformly distributed in formation, equal to initial pressure (p_i).

3. Mathematical Model

3.1. Establishment of Mathematical Model. The nonlinear governing equation of fluid flow in the radial cylindrical system is

$$\frac{\partial^2 p_f}{\partial r^2} + \frac{1}{r}\frac{\partial p_f}{\partial r} + C_\rho \left(\frac{\partial p_f}{\partial r}\right)^2 + \alpha_m \frac{k_m}{k_f}\left(p_m - p_f\right) = \frac{\mu \phi_f C_{ft}}{3.6 k_f}\frac{\partial p_f}{\partial t}, \tag{1}$$

$$-\alpha_m \left(p_m - p_f\right) = \frac{\mu \phi_m C_{mt}}{3.6 k_m}\frac{\partial p_m}{\partial t}, \tag{2}$$

where r is radial cylindrical coordinate; k_m is matrix permeability, μm^2; k_f is fracture permeability, μm^2; p_m is matrix pressure, MPa; p_f is fracture pressure, MPa; μ is viscosity, mPa·s; ϕ_m is matrix porosity, fraction; ϕ_f is fracture porosity, fraction; C_ρ is liquid compressibility, MPa^{-1}; C_{mt} is total compressibility of rock and liquid of matrix system, MPa^{-1}; C_{ft} is total compressibility of rock and liquid of fracture system, MPa^{-1}; α_m is geometric shape factor of matrix block, m^{-2}; t is well production time, h; the subscripts "m" and "f" represent "matrix" and "fracture," respectively.

The second power of the pressure gradient in (1) is called the quadratic pressure gradient term.

Initial condition is

$$p_m\big|_{t=0} = p_f\big|_{t=0} = p_i, \tag{3}$$

where p_i is initial formation pressure, MPa.

Well production condition at constant rate production based on effective radius is

$$\frac{k_f h}{\mu}\left(r\frac{\partial p_f}{\partial r}\right)\bigg|_{r=r_{wa}} = 1.842\times 10^{-3} qB + 0.04421 C_s \frac{\mathrm{d}p_w}{\mathrm{d}t}, \tag{4}$$

where B is fluid volume factor, dimensionless; C_s is wellbore storage coefficient, m^3/MPa; p_w is wellbore pressure, MPa; q is well rate at wellhead, m^3/d; r_{wa} is effective wellbore radius, m; h is formation thickness, m.

The effective wellbore radius r_{wa} is defined as [20]

$$r_{wa} = r_w \mathrm{e}^{-S}, \tag{5}$$

where r_w is real wellbore radius, m; S is skin factor, dimensionless:

$$\begin{aligned} &\lim_{r\to\infty} p = p_i \ \text{(infinite)}, \\ &p\big|_{r=r_e} = p_i \ \text{(constant pressure)}, \\ &\frac{\partial p}{\partial r}\bigg|_{r=r_e} = 0 \ \text{(closed)}, \end{aligned} \tag{6}$$

where r_e is external boundary radius, m.

The following dimensionless definitions are introduced to solve the mathematical model:

dimensionless radial distance $r_D = r/(r_w \mathrm{e}^{-S})$;

skin factor $S_t = k_f h \Delta p_s/(1.842\times 10^{-3} q\mu B)$; here Δp_s is additional pressure drop near wellbore;

dimensionless production time $t_D = 3.6 k_f t/(\phi \mu C_t r_w^2)$;

dimensionless fracture pressure $p_{fD} = k_f h(p_i - p_f)/(1.842\times 10^{-3} qB\mu)$;

dimensionless fracture pressure $p_{mD} = k_f h(p_i - p_m)/(1.842\times 10^{-3} qB\mu)$;

dimensionless wellbore storage coefficient $C_D = C_s/[6.2832 h r_w^2(\phi_f C_{ft} + \phi_m C_{mt})]$;

dimensionless time for dual media reservoir $t_D = 3.6 k_f t/[\mu r_w^2(\phi_f C_{ft} + \phi_m C_{mt})]$;

interporosity flow factor of matrix to fracture systems $\lambda_{mf} = \alpha_m r_w^2 (k_m/k_f)$;

fluid capacitance coefficient of fracture subsystem $\omega_f = \phi_f C_{ft}/(\phi_f C_{ft} + \phi_m C_{mt})$;

fluid capacitance coefficient of matrix subsystem $\omega_m = \phi_m C_{mt}/(\phi_f C_{ft} + \phi_m C_{mt})$, $\omega_f + \omega_m = 1$;

dimensionless coefficient of nonlinear term $\beta = 1.842\times 10^{-3} qB\mu C_\rho/(k_f h)$.

The dimensionless mathematical model is as follows.

The dimensionless governing equation of fluid flow in a radial cylindrical system is

$$\frac{\partial^2 p_{fD}}{\partial r_D^2} + \frac{1}{r_D}\frac{\partial p_{fD}}{\partial r_D} - \beta\left(\frac{\partial p_{fD}}{\partial r_D}\right)^2 + \lambda_{mf} e^{-2S}\left(p_{mD} - p_{fD}\right) = \omega_f e^{-2S}\frac{\partial p_{fD}}{\partial t_D}, \tag{7}$$

$$\lambda_{mf} e^{-2S}\left(p_{fD} - p_{mD}\right) = \omega_m e^{-2S}\frac{\partial p_{mD}}{\partial t_D}. \tag{8}$$

In real cases, β cannot be equal to 0 for the nonlinear flow model. If we take a limit of 0 to β ($\lim \beta \to 0$), the nonlinear model will be reduced to the conventional linear model.

Initial conditions are

$$p_{fD}\big|_{t_D=0} = p_{mD}\big|_{t_D=0} = 0. \tag{9}$$

Well production condition at constant rate is

$$C_D\frac{\partial p_{fD}}{\partial t_D}\bigg|_{r_D=1} - \left(r_D\frac{\partial p_{fD}}{\partial r_D}\right)\bigg|_{r_D=1} = 1. \tag{10}$$

External boundary conditions are

$$\begin{aligned} &\lim_{r_D\to\infty} p_{fD} = 0 \ \text{(infinite)}, \\ &p_{fD}\big|_{r_D=r_{eD}} = 0 \ \text{(constant pressure)}, \\ &\frac{\partial p_{fD}}{\partial r_D}\bigg|_{r_D=r_{eD}} = 0 \ \text{(closed)}. \end{aligned} \tag{11}$$

3.2. Solution to Dimensionless Mathematical Model. Because (7) is a nonlinear equation with two unknown functions of p_{fD} and p_{mD}, the first- and second-order derivatives of $\overline{p}_{fD}$ to r_D, the quadratic power of the first-order derivative, and the first-order derivative of $\overline{p}_{fD}$ to t_D, it is hard to linearize the nonlinear equation. Therefore, we have to seek the analytical solution of the nonlinear model in the other way.

We introduce the Laplace transform on the basis of t_D:

$$L\left[p_D\left(r_D, t_D\right)\right] = \overline{p}_D\left(r_D, u\right) = \int_0^\infty p_D\left(r_D, t_D\right) e^{-ut_D} dt_D, \tag{12}$$

where p_D is the variable in real space; $\overline{p}_D$ is the variable in Laplace space; t_D is the dimensionless time in real space; u is the time in Laplace space.

The dimensionless mathematical model in Laplace space is as follows.

The dimensionless governing equation of fluid flow in a radial cylindrical system is

$$\frac{\partial^2 \overline{p}_{fD}}{\partial r_D^2} + \frac{1}{r_D}\frac{\partial \overline{p}_{fD}}{\partial r_D} - \beta\left(\frac{\partial \overline{p}_{fD}}{\partial r_D}\right)^2 + \lambda_{mf} e^{-2S}\left(\overline{p}_{mD} - \overline{p}_{fD}\right) = u\omega_f e^{-2S}\overline{p}_{fD}, \tag{13}$$

$$\lambda_{mf} e^{-2S}\left(\overline{p}_{fD} - \overline{p}_{mD}\right) = u\omega_m e^{-2S}\overline{p}_{mD}. \tag{14}$$

By (14),

$$\overline{p}_{mD} = \frac{\lambda_{mf}}{u\omega_m + \lambda_{mf}}\overline{p}_{fD}. \tag{15}$$

Substituting (15) into (13),

$$\frac{\partial^2 \overline{p}_{fD}}{\partial r_D^2} + \frac{1}{r_D}\frac{\partial \overline{p}_{fD}}{\partial r_D} - \beta\left(\frac{\partial \overline{p}_{fD}}{\partial r_D}\right)^2 - f\left(u\right)\overline{p}_{fD} = 0, \tag{16}$$

$$f\left(u\right) = \left(\frac{\omega_m\lambda_{mf}}{u\omega_m + \lambda_{mf}} + \omega_f\right)ue^{-2S}. \tag{17}$$

If we set $\omega_f = 1$ and $\omega_m = 0$, the model is reduced to the single porosity medium (homogeneous) model, so (17) can be changed by

$$f\left(u\right) = ue^{-2S}. \tag{18}$$

In other words, under the same conditions of well production and formation boundary, the difference of dual-porosity model with homogeneous model in Laplace space only exhibits the function expression of $f(u)$, which means the flow governing equation of homogeneous model in Laplace space is also (16). Therefore if we obtain the solution of homogeneous model in Laplace space firstly, we will easily obtain the solution of dual-porosity model in Laplace space by changing the function of $f(u)$.

Because (16) is a nonlinear equation with $\overline{p}_{fD}$, the first- and second-order derivatives of $\overline{p}_{fD}$ to r_D, and the quadratic power of the first-order derivative in Laplace space, it is hard to linearize the nonlinear equation. Therefore, we have to seek the analytical solution of homogeneous model back to real space firstly.

For homogeneous model, the flow governing equation in real space can be expressed by

$$\frac{\partial^2 p_{fD}}{\partial r_D^2} + \frac{1}{r_D}\frac{\partial p_{fD}}{\partial r_D} - \beta\left(\frac{\partial p_{fD}}{\partial r_D}\right)^2 = e^{-2S}\frac{\partial p_{fD}}{\partial t_D}. \tag{19}$$

Well production and formation external boundary conditions are the same as (9)–(11).

The following variable modification [11, 16] is introduced to linearize (19):

$$p_{fD} = -\frac{1}{\beta}\ln\left(\chi + 1\right). \tag{20}$$

Then

$$\frac{\partial p_{fD}}{\partial r_D} = -\frac{1}{\beta}\frac{1}{(\chi+1)}\frac{\partial \chi}{\partial r_D},$$

$$\frac{\partial^2 p_{fD}}{\partial r_D^2} = \frac{1}{\beta(\chi+1)^2}\left(\frac{\partial \chi}{\partial r_D}\right)^2 - \frac{1}{\beta(\chi+1)}\frac{\partial^2 \chi}{\partial r_D^2},$$

$$\left(\frac{\partial p_{fD}}{\partial r_D}\right)^2 = \frac{1}{\beta^2}\frac{1}{(\chi+1)^2}\left(\frac{\partial \chi}{\partial r_D}\right)^2, \tag{21}$$

$$\frac{\partial p_{fD}}{\partial t_D} = -\frac{1}{\beta}\frac{1}{(\chi+1)}\frac{\partial \chi}{\partial t_D}.$$

Substitute (20)-(21) into (19), (9)–(11):

$$\frac{\partial^2 \chi}{\partial r_D^2} + \frac{1}{r_D}\frac{\partial \chi}{\partial r_D} = e^{-2S}\frac{\partial \chi}{\partial t_D},$$

$$\chi|_{t_D=0} = 0,$$

$$\left(\frac{\partial \chi}{\partial r_D} - C_D\frac{\partial \chi}{\partial t_D} - \beta\chi\right)\Big|_{r_D=1} = \beta,$$

$$\lim_{r_D\to\infty}\chi = 0 \ \text{(infinite)},$$

$$\chi|_{r_D=r_{eD}} = 0 \ \text{(constant pressure)}, \tag{22}$$

$$\left.\frac{\partial \chi}{\partial r_D}\right|_{r_D=r_{eD}} = 0 \ \text{(closed)}.$$

The homogeneous model in Laplace space via Laplace transform can be written by

$$\frac{\partial^2 \overline{\chi}}{\partial r_D^2} + \frac{1}{r_D}\frac{\partial \overline{\chi}}{\partial r_D} = f(u)\overline{\chi}, \qquad f(u) = ue^{-2S}, \tag{23}$$

$$\left.\frac{d\overline{\chi}}{dr_D}\right|_{r_D=1} - (uC_D - \beta)\overline{\chi}_w = \frac{\beta}{u}, \tag{24}$$

$$\lim_{r_D\to\infty}\overline{\chi} = 0 \ \text{(infinite)}, \tag{25}$$

$$\overline{\chi}|_{r_D=r_{eD}} = 0 \ \text{(constant pressure)}, \tag{26}$$

$$\left.\frac{\partial \overline{\chi}}{\partial r_D}\right|_{r_D=r_{eD}} = 0 \ \text{(closed)}, \tag{27}$$

where $\overline{\chi}$ is substitution variable of dimensionless fracture pressure in Laplace space and $\overline{\chi}_w$ is the value at the wall of wellbore ($r_D = 1$).

According to the previous derivation, we can obtain the following governing equation of dual-porosity model by changing $f(u)$ from (18) to (17) for (23):

$$\frac{\partial^2 \overline{\chi}}{\partial r_D^2} + \frac{1}{r_D}\frac{\partial \overline{\chi}}{\partial r_D} = f(u)\overline{\chi},$$

$$f(u) = \left(\frac{\omega_m\lambda_{mf}}{u\omega_m + \lambda_{mf}} + \omega_f\right)ue^{-2S}. \tag{28}$$

The general solution of (28) is

$$\overline{\chi} = AI_0\left(r_D\sqrt{f(u)}\right) + BK_0\left(r_D\sqrt{f(u)}\right). \tag{29}$$

Substitute (29) into (28) and (24):

$$I_0\left(\sqrt{f(u)}\right)\cdot A + K_0\left(\sqrt{f(u)}\right)\cdot B - \overline{\chi}_w = 0,$$

$$\sqrt{f(u)}I_1\left(\sqrt{f(u)}\right)\cdot A - \sqrt{f(u)}K_1\left(\sqrt{f(u)}\right) \tag{30}$$

$$\cdot B - (C_D u + \beta)\overline{\chi}_w = \frac{\beta}{u}.$$

Substitute (29) into (25)–(27):

$$\lim_{r_{eD}\to\infty} I_0\left(r_{eD}\sqrt{f(u)}\right)\cdot A + \lim_{r_{eD}\to\infty} K_0\left(r_{eD}\sqrt{f(u)}\right)\cdot B = 0,$$

$$I_0\left(r_{eD}\sqrt{f(u)}\right)\cdot A + K_0\left(r_{eD}\sqrt{f(u)}\right)\cdot B = 0,$$

$$I_1\left(r_{eD}\sqrt{f(u)}\right)\cdot A - K_1\left(r_{eD}\sqrt{f(u)}\right)\cdot B = 0, \tag{31}$$

where A and B are undetermined coefficients; $I_0()$ is modified Bessel function of the first kind, zero order; $I_1()$ is modified Bessel function of the first kind, first order; $K_0()$ is modified Bessel function of the second kind, zero order; $K_1()$ is modified Bessel function of the second kind, first order.

In (30)-(31), there are three unknown numbers (A, B, $\overline{\chi}_w$) and three equations, and solutions to the model in Laplace space can be easily obtained by using linear algebra, such as a Gauss-Jordan reduction.

In real space, χ_w and the derivative ($d\chi_w/dT_D$) can be obtained using a Stehfest numerical inversion [21] to convert $\overline{\chi}_w$ back to χ_w, and then dimensionless wellbore pressure (p_{wD}) and the derivative (dp_{wD}/dt_D) can be obtained by substituting χ_w into (20). The standard log-log type curves of well-test analysis of p_{wD} and ($p'_{wD}\cdot t_D/C_D$) versus t_D/C_D can then be obtained.

The difference of the nonlinear model with the conventional linear model is that the nonlinear model contains the quadratic gradient term; therefore the solutions of the linear and nonlinear models are different and the effect of the quadratic gradient term exhibits the difference of solutions in pressure transients and pressure derivative transients controlled by β. In the following, qualitative and quantitative analyses will be implemented to compare the solutions between the linear and nonlinear models.

4. Analysis of Nonlinear Flow Characteristics

4.1. Analysis of Nonlinear Flow Processes. Type curves reflect properties of underground formations. Type curves graphically show the process and characteristics of fluid flow in formations. Figures 1–4 show the type curves of pressure transients for well production in an underground dual-porosity media formation.

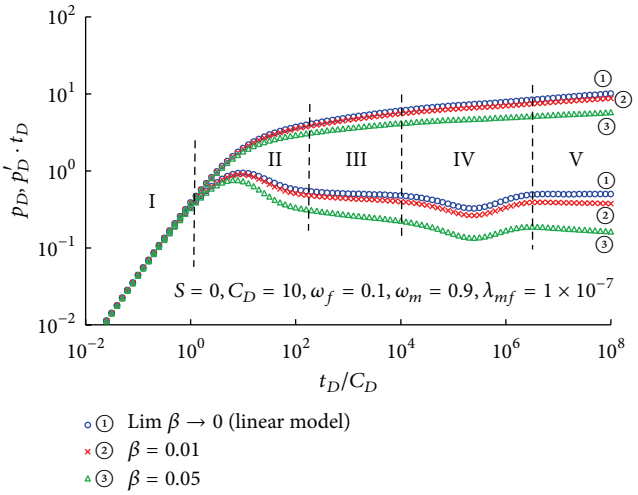

Figure 1: Type curves of pressure transients controlled by varying nonlinear coefficient (β).

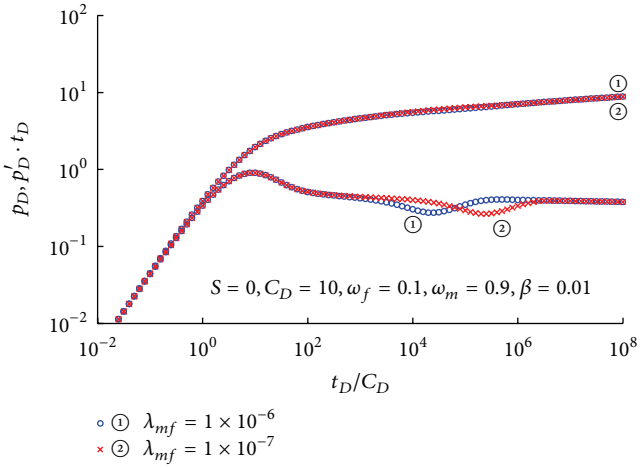

Figure 2: Type curves of pressure transients controlled by varying interporosity flow factor (λ_{mf}) for $\beta = 0.01$.

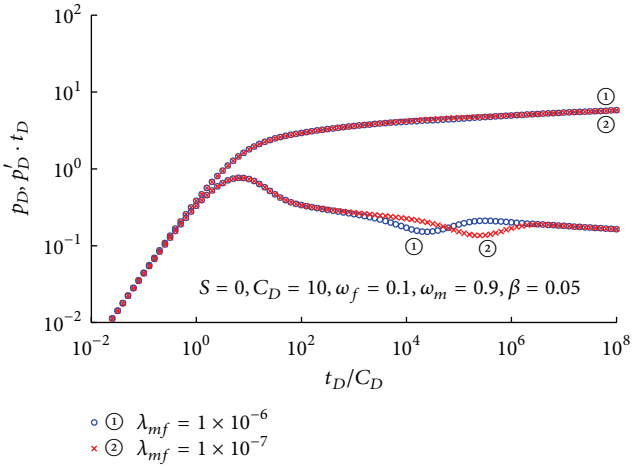

Figure 3: Type curves of pressure transients controlled by varying interporosity flow factor (λ_{mf}) for $\beta = 0.05$.

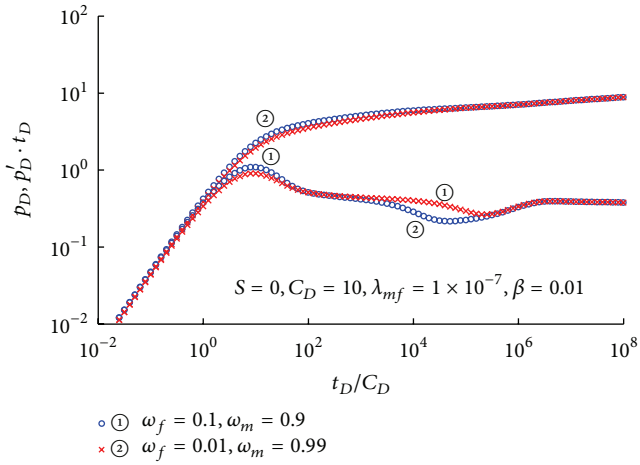

Figure 4: Type curves of pressure transients controlled by varying fluid capacitance coefficient (ω_m and ω_f) for $\beta = 0.01$.

Figure 1 shows the type curves of the nonlinear dual-porosity flow model with an infinite formation boundary. The pressure transients were simulated using a set of fixed parameters ($S = 0, C_D = 10, \omega_f = 0.1, \omega_m = 0.9, \lambda_{mf} = 1 \times 10^{-7}$) and a group of varying nonlinear term coefficients (β). The type curves were obviously controlled by β. Pressure transients were simulated by setting β as a limit of 0, 0.01, and 0.05. The curves of "lim $\beta \to 0$" are the curves associated with the conventional linear flow model (see the derivative curve ① in Figure 1). The nonlinearity of fluid flow influenced the pressure transients positively. Different formation has different value of β. We can calculate the value of β according to the definition of $\beta = 1.842 \times 10^{-3} qB\mu C_\rho/(k_f h)$, and usually the value of β varies from 0 to 0.05; therefore we simulated the type curves using 0.01 and 0.05 in the context.

Five main flow regimes can be observed.

(i) Regime I, pure wellbore storage regime: there are no differences in type curves between the linear and nonlinear models because fluid in formation does not start to flow and the influence of the nonlinear quadratic pressure gradient term is only produced for the flow in formation. Wellbore pressure transients are not affected by the nonlinearity of fluid flow in this regime.

(ii) Regime I, skin effect regime: there are little differences in type curves between the linear and nonlinear models. The curves of the nonlinear model gradually deviate from those of the linear model with time elapsing. The deviation of pressure derivative curve is more obvious than that of pressure curve for the same β. A larger β means a stronger nonlinearity on the type curves.

(iii) Regime III, early fracture radial regime: fluid in the fracture system of formation radially flows into the wellbore and the fluid in the matrix system of formation does not start to flow. The differences in type curves associated with the linear and nonlinear models are more obvious than those of regime II. A larger β results in a lager curve deviation of the nonlinear model from the linear model.

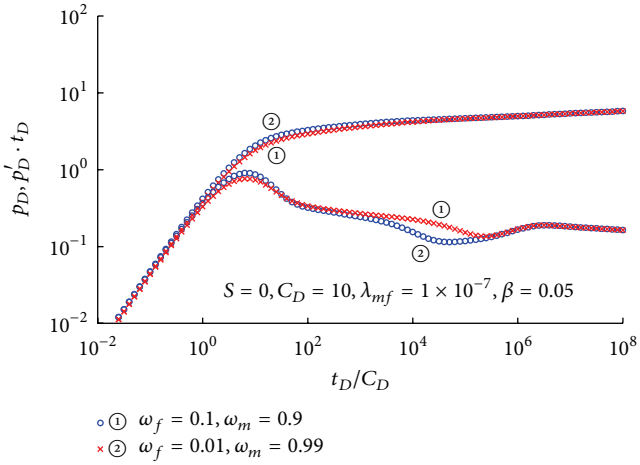

Figure 5: Type curves of pressure transients controlled by varying fluid capacitance coefficient (ω_m and ω_f) for $\beta = 0.05$.

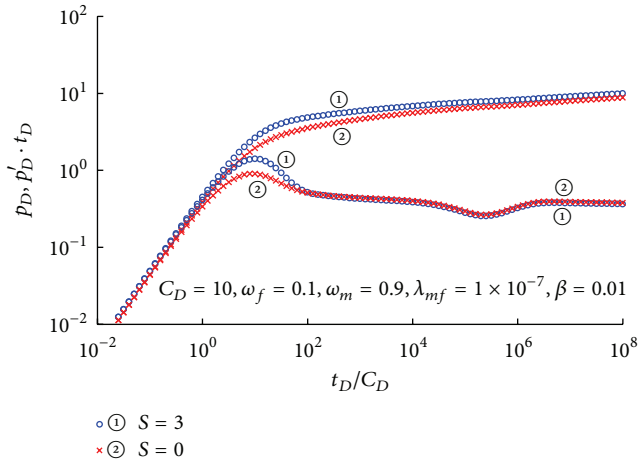

Figure 6: Type curves of pressure transients controlled by varying skin factor (S) for $\beta = 0.01$.

(iv) Regime IV, interporosity flow regime of matrix system to fracture system: the pressure derivative curve is V-shaped, which is the reflection of the interporosity flow of matrix to fracture. The differences in type curves associated with the linear and nonlinear models are more obvious than those of regimes II and III. The β influences the location of type curves more heavily.

(v) Regime V, whole radial flow stage of fracture and matrix systems: the interporosity flow regime had ended. The differences in type curves associated with the linear and nonlinear models are the most obvious among the five flow regimes. The differences increase with the increase of β. For conventional linear dual-porosity model, the slope of the pressure derivative curve in both regime III and regime V is zero; however, the pressure derivative curves of nonlinear dual-porosity model in regimes III and V are inclined instead of horizontal (see the derivative curves ② and ③ in Figure 1). As time elapsed, the pressure derivative curves of nonlinear model gradually deviate from the pressure derivative curve of linear model.

For constant pressure and closed boundaries, the type curves are similar to the nonlinear homogenous model of Guo and Nie [17] and are omitted here.

Except for nonlinear term coefficient (β), type curves are sensitive to the other model parameters.

Figures 2 and 3 reflect the shape characteristics of type curves affected by interporosity flow factor of fluid from matrix system to fracture system (λ_{mf}). The pressure transients were simulated using a set of fixed parameters ($S = 0, C_D = 10, \omega_f = 0.1, \omega_m = 0.9$) and changing λ_{mf} from 1×10^{-6} to 1×10^{-7}, respectively, for $\beta = 0.01$ and $\beta = 0.05$. Because λ_{mf} represents the starting time of interporosity flow of matrix system to fracture system, therefore the bigger the λ_{mf} is, the earlier the time of interporosity is, and as the value of λ_{mf} decreases, the V-shaped derivative curve moves right (see the derivative curves ① and ② in Figures 2 and 3).

Figures 4 and 5 reflect the shape characteristics of type curves affected by interporosity flow factor of fluid capacitance coefficients of fracture and matrix systems (ω_f and ω_m). The pressure transients were simulated using a set of fixed parameters ($S = 0, C_D = 10, \lambda_{mf} = 1 \times 10^{-7}$) and changing ω_f from 0.1 to 0.01 and ω_m from 0.9 to 0.99, respectively, for $\beta = 0.01$ and $\beta = 0.05$. Fluid capacitance coefficient of fracture system (ω_f) is coupled with fluid capacitance coefficient of fracture system (ω_m), and they represent the relative fluid storage capacitance for fracture and matrix systems, respectively. A greater ω_f is the response of relatively more reserves in fracture system. As ω_f decreases, the V-shaped derivative curve becomes deeper and wider (see the derivative curves ① and ② in Figures 4 and 5).

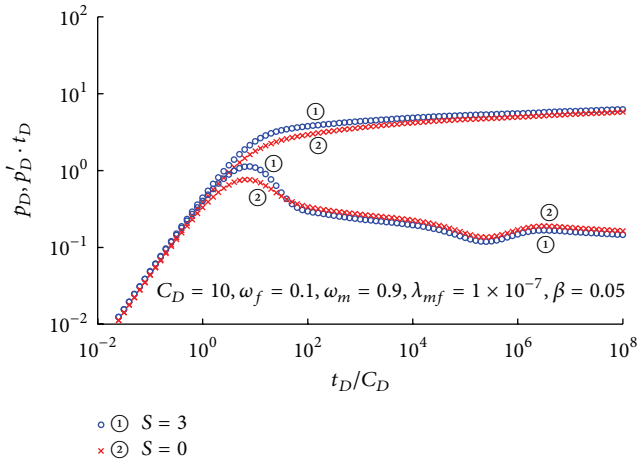

Figure 7: Type curves of pressure transients controlled by varying skin factor (S) for $\beta = 0.05$.

Figures 6 and 7 reflect the shape characteristics of type curves affected by skin factor of well (S). The pressure transients were simulated using a set of fixed parameters ($C_D = 10, \omega_f = 0.1, \omega_m = 0.9, \lambda_{mf} = 1 \times 10^{-7}$) and changing S from 3 to 0, respectively, for $\beta = 0.01$ and $\beta = 0.05$. Greater S leads to higher location of dimensionless pressure curve.

Table 1: Theoretical offset of type curves between the linear and nonlinear models ($\beta = 0.01$).

t_D/C_D	p_{wD}		DV	RDV (%)	$p'_{wD} \cdot (t_D/C_D)$		DV	RDV (%)
	Linear	Nonlinear			Linear	Nonlinear		
10^{-1}	0.0445	0.0445	0	0	0.0436	0.0436	0	0
10^{1}	1.9772	1.9397	0.0375	1.90	0.9454	0.9003	0.0451	4.77
10^{3}	4.9392	4.6066	0.3326	6.73	0.5076	0.4395	0.0681	13.42
10^{5}	7.0647	6.3938	0.6709	9.50	0.3588	0.2924	0.0664	18.51
10^{7}	8.9812	7.9242	1.0570	11.77	0.4995	0.3887	0.1108	22.18

Explanations: β = dimensionless coefficient of nonlinear term; t_D = dimensionless time; C_D = dimensionless wellbore storage coefficient; p_{wD} = dimensionless pressure; p'_{wD} = dimensionless pressure derivative; DV = differential value; RDV = relative differential value. Quantitative analysis of the nonlinear influence is made by setting β as 0.01, and the corresponding type curves (curves ②) are shown in Figure 1.

Table 2: Theoretical offset of type curves between the linear and nonlinear models ($\beta = 0.05$).

t_D/C_D	p_{wD}		DV	RDV (%)	$p'_{wD} \cdot (t_D/C_D)$		DV	RDV (%)
	Linear	Nonlinear			Linear	Nonlinear		
10^{-1}	0.0445	0.0445	0	0	0.0436	0.0435	0.0001	0.23
10^{1}	1.9772	1.7977	0.1795	9.08	0.9454	0.7385	0.2069	21.88
10^{3}	4.9392	3.6310	1.3082	26.49	0.5076	0.2695	0.2381	46.91
10^{5}	7.0647	4.6454	2.4193	34.24	0.3588	0.1528	0.2060	57.41
10^{7}	8.9812	5.4067	3.5745	39.80	0.4995	0.1814	0.3181	63.68

Explanations: β = dimensionless coefficient of nonlinear term; t_D = dimensionless time; C_D = dimensionless wellbore storage coefficient; p_{wD} = dimensionless pressure; p'_{wD} = dimensionless pressure derivative; DV = differential value; RDV = relative differential value. Quantitative analysis of the nonlinear influence is made by setting β as 0.01, and the corresponding type curves (curves ②) are shown in Figure 1.

4.2. Quantitative Analysis of Nonlinear Influence. "DV" and "RDV" are employed to show the quantitative differences between type curves [17, 19]:

$$\text{DV} = |\text{value of linear model} - \text{value of nonlinear model}|,$$
$$\text{RDV} = \frac{\text{DV}}{\text{value of linear model}} \times 100\%, \tag{32}$$

where DV is the differential value between linear and nonlinear models and RDV is the relative differential value between linear and nonlinear models.

Tables 1 and 2 show the quantitative differences of nonlinear influence on type curves for "$\beta = 0.01$" and "$\beta = 0.05$," respectively. Dimensionless pressure values and dimensionless pressure derivative values in Tables 1 and 2 were calculated by fixing a group of parameters ($S = 0, C_D = 10, \omega_f = 0.1, \omega_m = 0.9, \lambda_{mf} = 1 \times 10^{-7}$), and the corresponding type curves (curves ② and ③) are shown in Figure 1. The tables show that dimensionless pressure and its derivative are different between linear and nonlinear models.

The following quantitative differences can be seen.

For "$\beta = 0.01$" (see Table 1): when "$t_D = 10^{-1}$" (regime I in Figure 1), DV and RDV of pressure are 0, and DV and RDV of pressure derivative are also 0; when "$t_D = 10^{1}$" (regime II in Figure 1), DV of pressure is 0.0375 and RDV of pressure is 1.90%, and DV of pressure derivative is 0.0451 and RDV of pressure derivative is 4.77%; when "$t_D = 10^{3}$" (regime III in Figure 1), DV of pressure is 0.3326 and RDV of pressure is 6.73%, and DV of pressure derivative is 0.0681 and RDV of pressure derivative is 13.42%; when "$t_D = 10^{5}$" (regime IV in Figure 1), DV of pressure is 0.6709 and RDV of pressure is 9.50%, and DV of pressure derivative is 0.0664 and RDV of pressure derivative is 18.51%; when "$t_D = 10^{7}$" (regime V in Figure 1), DV of pressure is 1.0570 and RDV of pressure is 11.77%, and DV of pressure derivative is 0.1108 and RDV of pressure derivative is 22.18%.

For "$\beta = 0.05$" (see Table 2): when "$t_D = 10^{-1}$" (regime I in Figure 1), DV and RDV of pressure are 0, and DV of pressure derivative is 0.0001 and RDV of pressure derivative is 0.23%; when "$t_D = 10^{1}$" (regime II in Figure 1), DV of pressure is 0.1795 and RDV of pressure is 9.08%, and DV of pressure derivative is 0.2069 and RDV of pressure derivative is 21.88%; when "$t_D = 10^{3}$" (regime III in Figure 1), DV of pressure is 1.3082 and RDV of pressure is 26.49%, and DV of pressure derivative is 0.2381 and RDV of pressure derivative is 46.91%; when "$t_D = 10^{5}$" (regime IV in Figure 1), DV of pressure is 2.4193 and RDV of pressure is 34.24%, and DV of pressure derivative is 0.2060 and RDV of pressure derivative is 57.41%; when "$t_D = 10^{7}$" (regime V in Figure 1), DV of pressure is 3.5745 and RDV of pressure is 39.80%, and DV of pressure derivative is 0.3181 and RDV of pressure derivative is 63.68%.

As shown in the tables, DV and RDV increase with an increase in elapsed time. The RDV of pressure derivative is larger than that of pressure at a fixed time, such as the fact that when "$t_D/C_D = 10^{3}$" for "$\beta = 0.01$" in Table 1, RDV of pressure derivative is 13.42%, which is greater than that of pressure (6.73%). It can be observed from the tables that DV and RDV increase with an increase in β, such as the fact that when "$t_D/C_D = 10^{3}$" RDV of pressure for "$\beta = 0.01$" is 6.73% and RDV of pressure for "$\beta = 0.05$" is 26.49%.

In general, qualitative and quantitative analyses show that the nonlinearity caused by the quadratic pressure gradient term influences the pressure transients positively.

5. Conclusions

A nonlinear flow model for well production in an underground dual-porosity media formation was derived. The transient flow behavior caused by well production was modeled. The type curves of pressure transients simulated using different values of model parameters showed the nonlinear dual-porosity processes and reflected the differences between nonlinear and linear models. The nonlinear term in the flow equation is suggested to be retained.

Conflict of Interests

The authors declare that there is no conflict of interests regarding the publication of this paper.

Acknowledgments

The authors would like to acknowledge NSFC (National Natural Science Foundation of China) for supporting this paper through a Project (no. 51304164)—Research on the Pressure Dynamics of Multiple-Acidized-Fractured Horizontal Wells in Fractured-Vuggy Carbonate Formations. The paper also was financially supported by 973 Program (National Basic Research Program) of China under Grant no. 2014CB239205 and a basic research project under Grant no. 2015JY0132 from Science and Technology Department of Sichuan Province. The authors would also like to thank the reviewers and editors whose critical comments were very helpful in preparing this paper.

References

[1] J. Finjord, "A solitary wave in a porous medium," *Transport in Porous Media*, vol. 5, no. 6, pp. 591–607, 1990.

[2] D. Giachetti and G. Maroscia, "Existence results for a class of porous medium type equations with a quadratic gradient term," *Journal of Evolution Equations*, vol. 8, no. 1, pp. 155–188, 2008.

[3] Y. Liang, J. D. Price, D. A. Wark, and E. B. Watson, "Nonlinear pressure diffusion in a porous medium: approximate solutions with applications to permeability measurements using transient pulse decay method," *Journal of Geophysical Research B: Solid Earth*, vol. 106, no. 1, pp. 529–535, 2001.

[4] J. Finjord and B. S. Aadnoy, "Effects of the quadratic gradient term in steady-state and semisteady-state solutions for reservoir pressure," *SPE Formation Evaluation*, vol. 4, no. 3, pp. 413–15969, 1989.

[5] Y. Wang and M. B. Dusseault, "The effect of quadratic gradient terms on the borehole solution in poroelastic media," *Water Resources Research*, vol. 27, no. 12, pp. 3215–3223, 1991.

[6] C. Chakrabarty, S. M. F. Ali, and W. S. Tortike, "Analytical solutions for radial pressure distribution including the effects of the quadratic-gradient term," *Water Resources Research*, vol. 29, no. 4, pp. 1171–1177, 1993.

[7] C. Chakrabarty, S. M. F. Ali, and W. S. Tortike, "Effects of the nonlinear gradient term on the transient pressure solution for a radial flow system," *Journal of Petroleum Science and Engineering*, vol. 8, no. 4, pp. 241–256, 1993.

[8] M. Bai, Q. Ma, and J.-C. Roegiers, "A nonlinear dual-porosity model," *Applied Mathematical Modelling*, vol. 18, no. 11, pp. 602–610, 1994.

[9] M. Bai and J. C. Roegiers, "On the correlation of nonlinear flow and linear transport with application to dual-porosity modeling," *Journal of Petroleum Science and Engineering*, vol. 11, no. 2, pp. 63–72, 1994.

[10] T. A. Jelmert and S. A. Vik, "Analytic solution to the nonlinear diffusion equation for fluids of constant compressibility," *Journal of Petroleum Science and Engineering*, vol. 14, no. 3-4, pp. 231–233, 1996.

[11] A. S. Odeh and D. K. Babu, "Comparison of solutions of the nonlinear and linearized diffusion equations," *SPE Reservoir Engineering*, vol. 3, no. 4, pp. 1202–1206, 1988.

[12] S. Braeuning, T. A. Jelmert, and S. A. Vik, "The effect of the quadratic gradient term on variable-rate well-tests," *Journal of Petroleum Science and Engineering*, vol. 21, no. 3-4, pp. 203–222, 1998.

[13] X. L. Cao, D. K. Tong, and R. H. Wang, "Exact solutions for nonlinear transient flow model including a quadratic gradient term," *Applied Mathematics and Mechanics*, vol. 25, no. 1, pp. 102–109, 2004.

[14] D.-K. Tong and R.-H. Wang, "Exact solution of pressure transient model for fluid flow in fractal reservoir including a quadratic gradient term," *Energy Sources*, vol. 27, no. 13, pp. 1205–1215, 2005.

[15] S. L. Marshall, "Nonlinear pressure diffusion in flow of compressible liquids through porous media," *Transport in Porous Media*, vol. 77, no. 3, pp. 431–446, 2009.

[16] R. S. Nie and Y. Ding, "Research on the nonlinear spherical percolation model with quadratic pressure gradient and its percolation characteristics," *Natural Science*, vol. 2, no. 2, pp. 98–105, 2010.

[17] J. C. Guo and R. S. Nie, "Nonlinear flow model for well production in an underground formation," *Nonlinear Processes in Geophysics*, vol. 20, no. 3, pp. 311–327, 2013.

[18] M. Dewei, J. Ailin, J. Chengye, Z. Qian, and H. Dongbo, "Research on transient flow regulation with the effect of quadratic pressure gradient," *Petroleum Science and Technology*, vol. 31, no. 4, pp. 408–417, 2013.

[19] X.-L. Wang, X.-Y. Fan, Y.-M. He, R.-S. Nie, and Q.-H. Huang, "A nonlinear model for fluid flow in a multiple-zone composite reservoir including the quadratic gradient term," *Journal of Geophysics and Engineering*, vol. 10, no. 4, Article ID 045009, 2013.

[20] R. G. Agarwal, R. Al-Hussainy, and H. J. Ramey Jr., "An investigation of wellbore storage and skin effect in unsteady liquid flow: I. Analytical treatment," *Society of Petroleum Engineers Journal*, vol. 10, no. 3, pp. 279–290, 1970.

[21] H. Stehfest, "Numerical inversion of Laplace transform—algorithm 368," *Communication of the ACM*, vol. 13, no. 1, pp. 47–49, 1970.